On the Interpolation of a Vector Field

JOSEPH T. SCHAEFER AND CHARLES A. DOSWELL III

Techniques Development Unit, National Severe Storms Forecast Center, Kansas City, MO 64106

(Manuscript received 6 October 1978, in final form 2 January 1979)

ABSTRACT

By its very nature, interpolation in a vector field is ambiguous, owing to the somewhat arbitrary nature of the vector norm. Since a two-dimensional vector field can be specified by two scalar quantities, which can be separately interpolated, the ambiguity can be resolved by forcing the interpolated wind field to preserve the vorticity and divergence fields associated with the raw data. A method to calculate divergence and vorticity directly from randomly spaced wind observations is developed and, using analytically generated data, shown to produce more accurate results than conventional computations. Two methods of retrieving the wind field from the analyzed scalar fields are presented and also tested on the analytic field. Finally, total analysis, from wind observations to gridded wind fields, is demonstrated on real meteorological data.

1. Introduction

A fundamental problem in numerical analysis is that of non-uniqueness of vector field interpolation (Levinson and Redheffer, 1970, p. 409). This arises since a vector is a directed quantity; interpolation of components does not necessarily yield the same results as interpolation of magnitude and direction. This problem can have a significant impact on objective interpolation of the meteorological wind field. For a simple demonstration, consider two points on an east-west line (Fig. 1). At point A the horizontal wind is westerly (270°) at 10 m s^{-1} while at point C it is southerly (180°) at 10 m s^{-1}. The interpolated wind speed at the midpoint (B) is also 10 m s^{-1} from a direction of 225°. However, component interpolation gives a reconstructed wind which has a speed of 7.07 m s^{-1}, again from a direction of 225°. An example of this interpolation problem's effect has been shown by Williams (1976). In a comparison of data interpolated via computer to that interpolated manually, he found that while the two methods yielded virtually equivalent values for scalar quantities (e.g., temperature, pressure, dewpoint temperature), the wind speed estimates differed by an average of 3.5 m s^{-1}, while wind directions were roughly equivalent.

For simplicity, this discussion is limited to the horizontal wind, a two-dimensional vector field. Such vectors can be uniquely defined, to within a vector constant, by the velocity potential and streamfunction (Schwartz *et al.*, 1960, p. 326). The velocity potential represents the irrotational component of the vector field while the streamfunction corresponds to the nondivergent portion of it. The horizontal divergence of the wind and appropriate boundary conditions determine the velocity potential. Similarly, the vertical component of vorticity is used to find the streamfunction, again under the boundary conditions. Since these are scalars, any of a wide variety of interpolation schemes can be applied to them (e.g., Doswell, 1977).

Certain aspects of this approach have been examined by Ceselski and Sapp (1975). However, their presentation does not emphasize the details concerning the technique used to determine "measured" vorticity and divergence and does not objectively assess the quality of the results. Rather, they have concentrated on the interpolation methods. Further, we feel that determination of reconstructed winds from the resulting divergence and vorticity fields requires additional examination.

The wind recovery process intimately depends upon the proper specification of boundary conditions. Several papers have discussed this problem (e.g., Stephens, 1968; Hawkins and Rosenthal, 1965; Bedient and Vederman, 1964; Sangster, 1960). The essence of these works is that specification of boundary conditions (Dirichlet, Neumann or mixed) on streamfunction and velocity potential predetermines the structural details of the wind field, to some degree.

Two different inversion techniques based on variational methods are presented here. The first requires the wind field to have the specified divergence and vorticity, subject to the constraint that the domain-averaged velocity of the analyzed field equals that obtained through a prior component interpolation. The second method forces the wind field's divergence and vorticity to be as close to

the predetermined values as is possible, under the restriction that the winds around the boundary have a point-by-point correspondence to those obtained by some independent interpolation technique.

2. Direct evaluation of divergence and vorticity

a. Advantages of integral definition

From a generalization of Stokes' Theorem, the horizontal divergence can be computed either by differentiation or by integration:

$$D \equiv \nabla_H \cdot \mathbf{v} \equiv \frac{\partial u}{\partial x} + \frac{\partial v}{\partial y} \equiv \lim_{A \to 0} \frac{1}{A} \oint_\Gamma \mathbf{k} \cdot \mathbf{v} \times d\mathbf{r}, \quad (1)$$

where $A = \iint_S d\sigma$ is the area of the surface S, $\mathbf{k}$ a unit vector normal to S, $d\sigma$ a differential surface area, and $d\mathbf{r}$ the differential of the position vector along the curve Γ which bounds S and lies in the horizontal plane. In applying the differential definition to real data, many problems arise. As pointed out in Section 1, interpolation of winds to a uniform grid is a non-unique process. Further, a conventional centered difference always underestimates the true derivative [via multiplication by a diffraction function, as shown by Hamming (1962, p. 318)]. A third error source stems from the limited accuracy of the data itself. Morel and Necco (1973) have shown that the total uncertainty of the computation can be greater than 100%.

The integral definition eases these constraints. Since line integrals are being evaluated, an initial interpolation of the winds is not necessary. Rather, it is assumed that an individual wind measurement represents an average value along a portion of the path of integration. Also, the "roughing" inherent in numerical differentiation is replaced by the "smoothing" of integration. However, the increased number of "data points" available (Ceselski and Sapp, 1975) allows a compensating resolution increase in the interpolated fields. While there is still uncertainty in the computations, Eddy (1964) has concluded that the noise level in the meteorologically important part of the spectrum is significantly less than the true value. It must be pointed out that the limit in the defining equation implies that the computed divergence is the average value within the spatial curve considered and not a true point value. Thus, a horizontal scale is attached to each estimate. Morel and Necco (1973) have shown that the spectrum is adequately measured for wave lengths greater than about 400 km (the approximate spacing between rawinsondes over the contiguous United States).

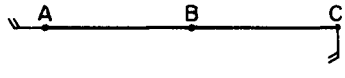

FIG. 1. Schematic example of non-uniqueness problem in vector interpolation.

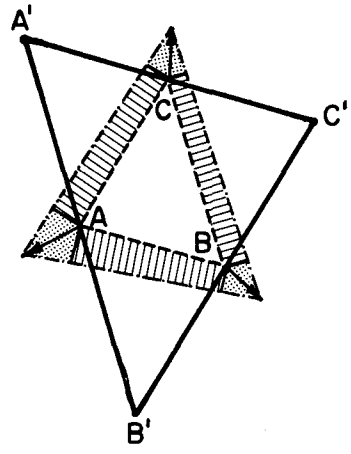

FIG. 2. Geometric configuration for three different methods of evaluating the line integral definitions (see text for details).

The vertical component of vorticity can be similarly defined through an integration procedure:

$$\xi \equiv \mathbf{k} \cdot \nabla \times \mathbf{v} \equiv \frac{\partial v}{\partial x} - \frac{\partial u}{\partial y} \equiv \lim_{A \to 0} \frac{1}{A} \oint_\Gamma \mathbf{v} \cdot d\mathbf{r}. \quad (2)$$

Since the rotation of wind vectors 90° to the right produces a wind field with vorticity equal to the divergence of the original field (Saucier, 1955, p. 339), comments on the divergence estimates are directly applicable to vorticity, and evaluation techniques are similar.

b. Method of evaluation

Bellamy (1949) has developed a method of estimating divergence via an integral technique. For the curve Γ, a triangle is selected with vertices at the wind observation points (points A, B, C, in Fig. 2). The winds are then allowed to displace the vertices for a time interval δt. Since divergence is equal to the percentage increase in area enclosed by the curve per unit time, an estimate of its value is immediately obtained. This method assumes that the wind varies linearly along each leg of the triangle.

Under the linearity assumption, a direct evaluation of the line integrals in Eqs. (1) and (2) is possible. The mean wind along each leg of the triangle is considered to be the component average of the values at the two vertices. It is informative to note that this divergence estimate differs from that obtained by the Bellamy method. Direct evaluation of the line integral yields a change in area equal to the hatched portions in the figure. The Bellamy method considers not only this expansion, but also an additional area around each vortex (stippled portions of figure). The magnitude of the difference between these results is directly proportional to the time

increment δt chosen for the Bellamy method. As δt approaches zero, the two methods converge to the same answer.

A third method of evaluation is available. A "circumscribed" triangle can be constructed (points A′, B′, C′ in Fig. 2) so that wind observations are located at the mid-point of each leg. When this is done, it is no longer necessary to compute an "average" wind along each segment. Rather, the mean wind along a side is approximated by the only wind measured along it. This is obviously crude, but it makes maximum use of observed data, reserving filtering and smoothing to the interpolation scheme used to grid the randomly spaced data, where the response can be spectrally controlled. Evaluation of the line integral is straightforward, with results virtually identical to those of the second method above.

It should also be noted that the derivative and integral evaluations of the divergence (vorticity) are equivalent, to within an approximation involving the determination of an "average" wind vector. To see this, we consider a centered finite difference scheme, so that

$$\nabla\cdot\mathbf{v}\big|_1 \approx \frac{u_3-u_5}{2\Delta x}+\frac{v_4-v_2}{2\Delta y}=\frac{(u_3-u_5)(2\Delta y)+(v_4-v_2)(2\Delta x)}{4\Delta x\Delta y}\approx\frac{1}{A}\oint \mathbf{k}\cdot\mathbf{v}\times d\mathbf{r}, \tag{3}$$

$$\mathbf{k}\cdot\nabla\times\mathbf{v}\big|_1 \approx \frac{v_3-v_5}{2\Delta x}-\frac{u_4-u_2}{2\Delta y}=\frac{(u_2-u_4)(2\Delta x)+(v_3-v_5)(2\Delta y)}{4\Delta x\Delta y}\approx\frac{1}{A}\oint \mathbf{v}\cdot d\mathbf{r}, \tag{4}$$

where the grid is arranged as indicated in Fig. 3. In applying the derivative definition, it is tacitly assumed that the mean wind along the path connecting three grid points is equal to the wind at the center point (e.g., the average wind along the path connecting points 6 and 7 equals v_3). This may not be true. The smoothing process used by the National Meteorological Center model (Shuman and Hovermale, 1968) changes this implied averaging of the wind by effectively assuming that the mean wind along a path is obtained with a Hann average (Blackman and Tukey, 1958, p. 171).

Both theoretical and practical considerations limit the triangles for which divergence computations can be reliably made. From a large set of wind observations, a much larger set of triangles can be obtained. The process of choosing a particular subset of triangles from the set of all possible triangles has an influence on the divergence calculation, since the computed divergence values are not independent. Instead, each represents an average divergence over its associated triangle, which shares at least one side with adjacent triangles. Ideally, uniform triangle sizes should be used. Further, they should have an area commensurate with that of the grid used in the final objective analysis (Eddy, 1964). Since evaluation of the line integral becomes unstable when the data are unevenly distributed with respect to the centroid, the ideal triangles should be equilateral.

For real meteorological data, none of these requirements can be precisely satisfied, but they are used as constraints in selecting which triangles to consider. In a manner somewhat similar to Celselski and Sapp (1975), an initial circle is drawn around each wind observation. Within that circle, the number of wind observations is counted. The radius of the circle is then systematically varied until at least four but less than nine observations (to limit the possible triangles within the circle to a reasonable number) are contained within it. All combinations of the selected observations are then used to construct candidate triangles. Candidate triangles may overlap, and do not have to include the central observation point. From geometric considerations, any triangle containing an arbitrarily chosen minimum angle of 15° or less is immediately discarded.

The remaining triangles are each assigned a weight equal to the square of the tangent of the minimum angle, divided by the area. This empirically motivated weight has the feature that for similar triangles, the one with the smallest area has the largest weight. For equal area triangles, the one closest to being equilateral will be weighted most. It should be emphasized that this weighting is not used in the interpolation, but is only done to choose those candidate triangles which are closest to being ideal. Within each scanning circle, the maximum number of triangles retained is arbitrarily set at two more than the number of data points it contains.

From these triangles, the line integrals are evaluated. A divergence (or vorticity) value is computed at each triangle centroid. These values are considered as observations and interpolated to a uniform grid. The grid, shown in Fig. 4, is chosen such that its spacing is roughly half that of the average data spacing. This results in each grid point representing an area about the size of the smallest candidate triangles.

c. Test of technique on an analytically defined field

To show the validity of the technique, a procedure similar to that of Leary and Thompson (1973)

is employed. An analytic wind field (thus having known divergence and vorticity) is defined. Wind values at locations corresponding to the actual rawinsonde observing stations (Fig. 4) are used to evaluate the line integrals for divergence and vorticity. Wind components, divergence and vorticity are objectively interpolated to equally spaced grid points. Interpolated wind components are used to evaluate the differential definition of the derived fields via centered differences.

A one-pass Gaussian weighting (Barnes, 1964) has been chosen for interpolation. While arguments exist in favor of other interpolation techniques, this choice does not detract from the generality of the conclusions. If fields computed using the integral technique are substantially better than those obtained through differentiation when a simple interpolation method is employed, the increased "resolution" available (because there are more triangles than wind observations) should make even greater improvement possible when more exotic objective analysis techniques are used.

A synoptic time (1200 GMT 8 November 1977) has been selected more or less at random. For this time, 85 rawinsondes were released in and around the analysis grid. From these observations, 333 triangles were retained by the selection routine.

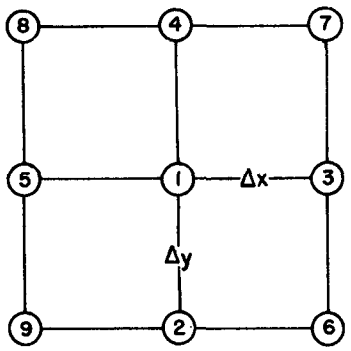

FIG. 3. Arrangement of a centered finite difference grid (see text for details).

For the first test, a Rankine-combined vortex (Milne-Thomson, 1968, p. 355) centered in Kansas (the approximate center of the data-rich contiguous United States) is defined over the analysis grid. For such a flow field, the product of vorticity and the two metrical coefficients (modified vorticity) is a circular disk of constant value, with zero values elsewhere. The modified vorticity field is also indicated on Fig. 4. The divergence is identically zero.

When divergence is computed via the differential definition, nine relatively strong centers ($|D|$

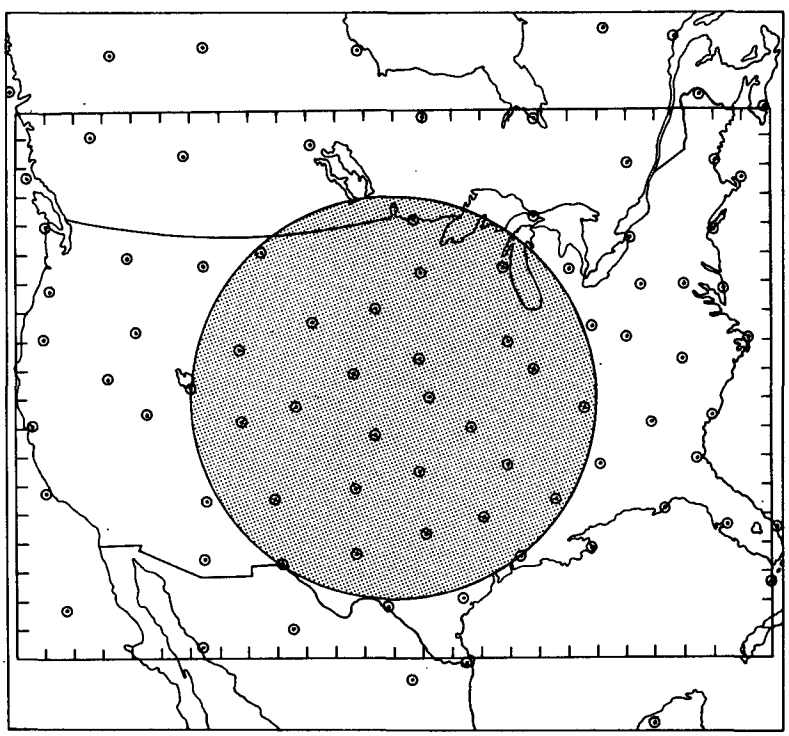

FIG. 4. 50 kPa rawinsonde observing sites at 1200 GMT 8 November 1977, with superimposed analysis grid. Shaded circle denotes region of constant modified vorticity (2.99×10^{-5} s^{-1}). Tick marks indicate the coordinates of the grid.

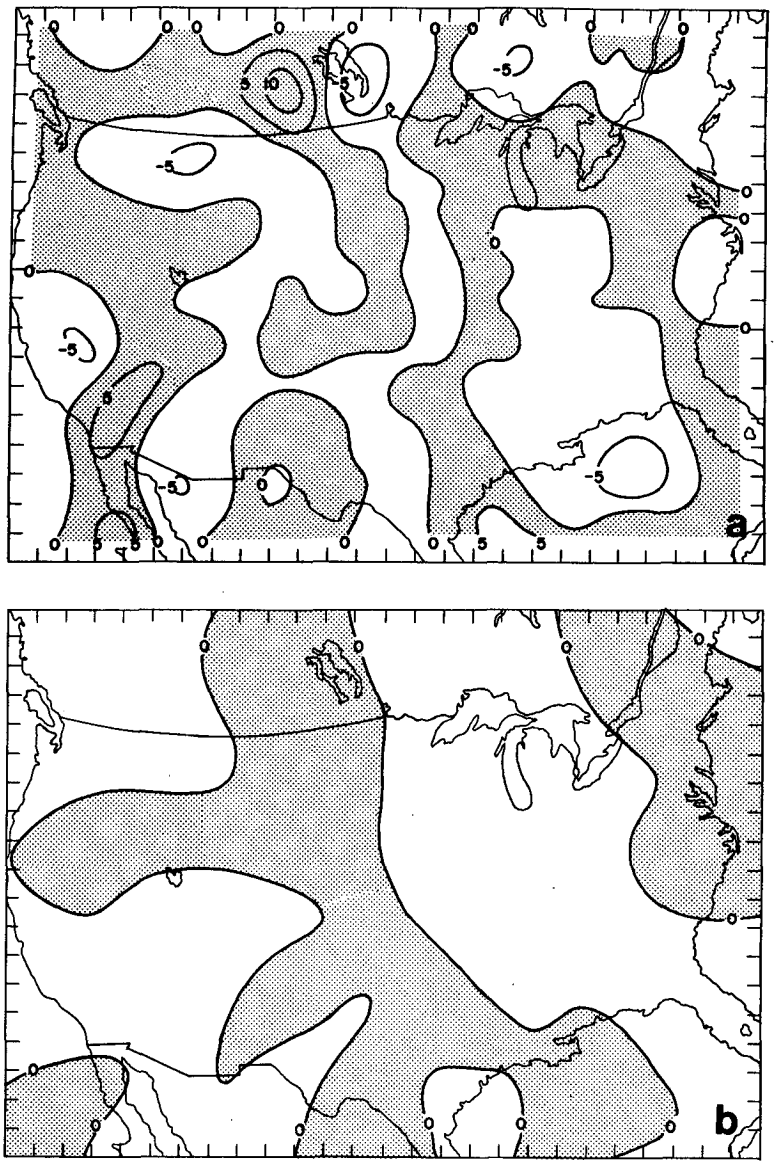

FIG. 5. Divergence times 10^{-6} s^{-1}; shading denotes positive values. (a) Differential definition from component analysis, (b) direct evaluation via line integral.

$> 5 \times 10^{-6}$ s^{-1}) are fallaciously created (Fig. 5a). In contrast, the line integral evaluation yields no values of this magnitude (Fig. 5b) and essentially shows numerical noise superposed on the zero divergence field.

A dramatic alteration of the modified vorticity field occurs when the differentiation process is employed (Fig. 6a). The uniform core is broken into three distinct centers with very noticeable wave-like perturbations developing along the theoretically circular boundary. While line integration does not yield a perfect observation of the field (Fig. 6b), its representation is much closer to actuality. Only one maximum is present and its general shape is more nearly circular. Thus, for the Rankine-combined vortex, the integral evaluation gives a substantial improvement in the estimation of kinematic parameters.

As a further test, a mathematical streamfunction which resembles atmospheric flow (Miyakoda, 1963) is examined:

$$\psi(x,y) = C - Uy - Vy^2 + Wy^3 + A \sin(x) + B \cos(2x) - E \cos(x) \sin(y) - D\{1 + [(x - x_0)^2 + (y - y_0)^2]/L^2\}^{-1/2}, \quad (5)$$

where C, U, V, W, A, B, E, D, L, x_0 and y_0 are constants. Since this is a stream function, there is

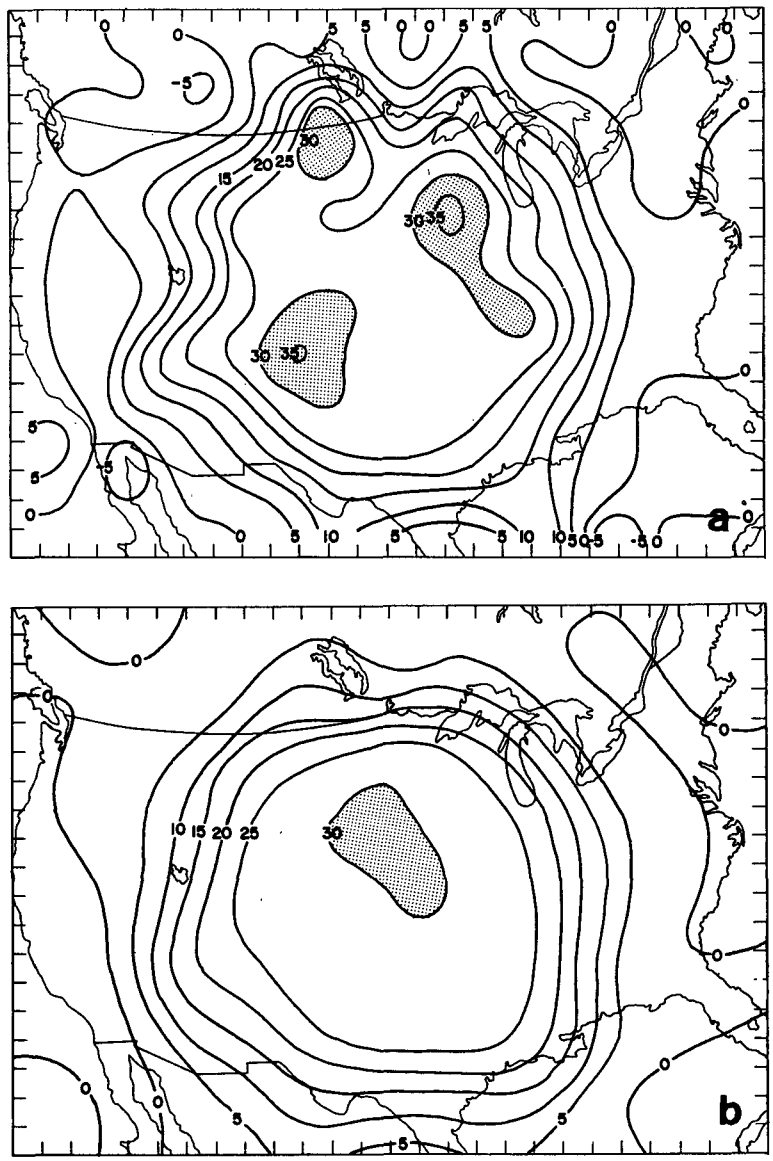

FIG. 6. Vorticity times 10^{-6} s^{-1}; shading denotes areas in excess of 30 $\times$ 10^{-6} s^{-1}. (a) Differential definition from component analysis, (b) direct evaluation via line integral.

no divergence in the associated winds. For one choice of the constants,[1] the streamfunction and its associated vorticity field are shown in Fig. 7. Winds implied by this streamfunction are computed at the rawinsonde observing sites, and divergence and vorticity are evaluated by both line integral and derivative techniques. In neither case is the computed divergence field (Fig. 8) equal to the true (zero) field. However, the triangle method gives a marked improvement over the component technique in the depiction. While ten centers of relatively strong divergence are created by the differential evaluation, only three such centers are present in the integral depiction. Further, the magnitudes obtained by using the triangles are considerably smaller than those found when the other method is applied.

The discrepancies between the true vorticity field and those computed by either of the two methods (Fig. 9) are quite noticeable. Both methods of evaluation show a reduction of about 25% in the amplitude of the vorticity. This reduction is a direct result of the interpolation's spectral characteristics and is not of concern here. There are

[1] The particular choice of constants depends on the grid geometry, so that the actual values chosen are not of general significance and have not been presented.

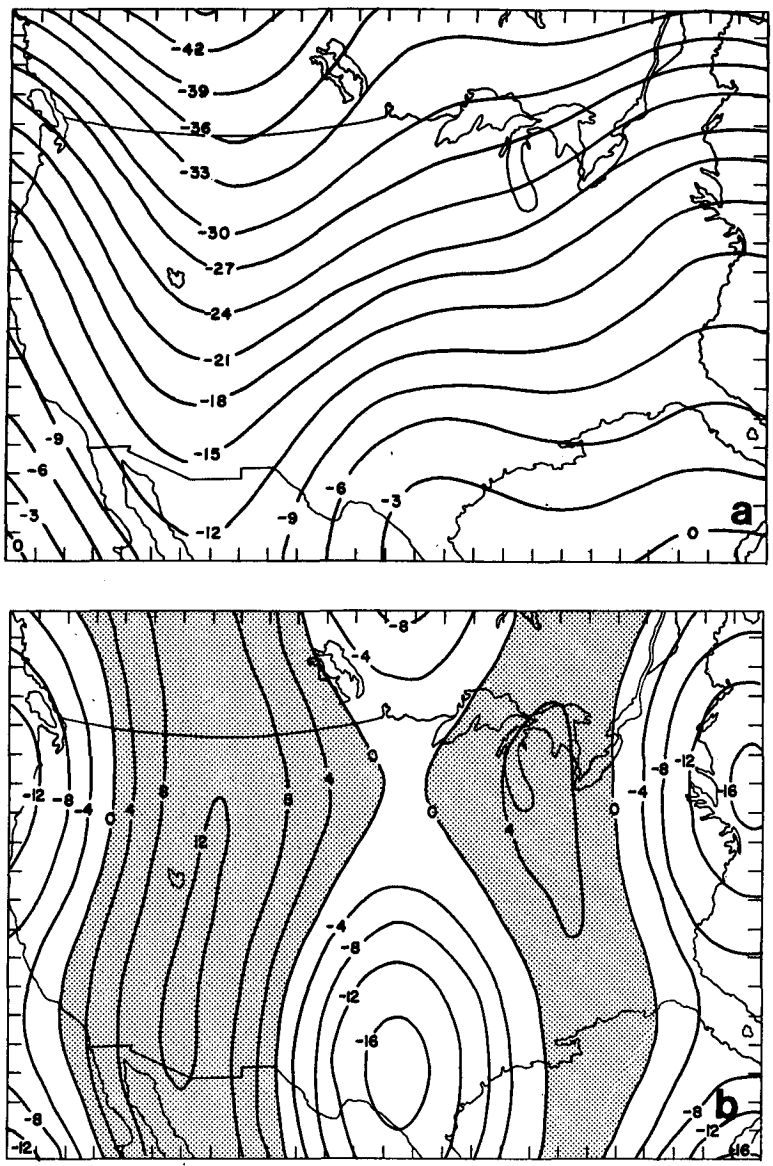

FIG. 7. Theoretical field for one specification of the constants in Eq. (5). (a) Streamfunction times 10^6 m^2 s^{-1}, (b) Vorticity in units of 2.5×10^{-6} s^{-1}.

indications of the banded vorticity pattern in both analyses, but the structural details differ significantly. Along the east side of the major trough, the component definition yields two distinct centers, one on either side of the true maximum, rather than one elongated maximum approximately in the mid-portions of the positive band. Also, this technique locates a relative minimum right in the middle of the actual maximum. A similar phenomenon occurs in the weaker positive vorticity area over the eastern portion of the grid where the one true maximum is broken into three portions (only two are shown, owing to the contour interval chosen). In contrast, the line integral technique preserves the existence of a single maximum within both regions.

In general, these examples point out that, while neither evaluation technique produces a perfect analysis of the vorticity and divergence fields, the integral method produces a pattern which is much more consistent with the actual field. This enhancement in the analysis stems directly from the easing of assumptions implicit in the evaluation of the kinematic quantities.

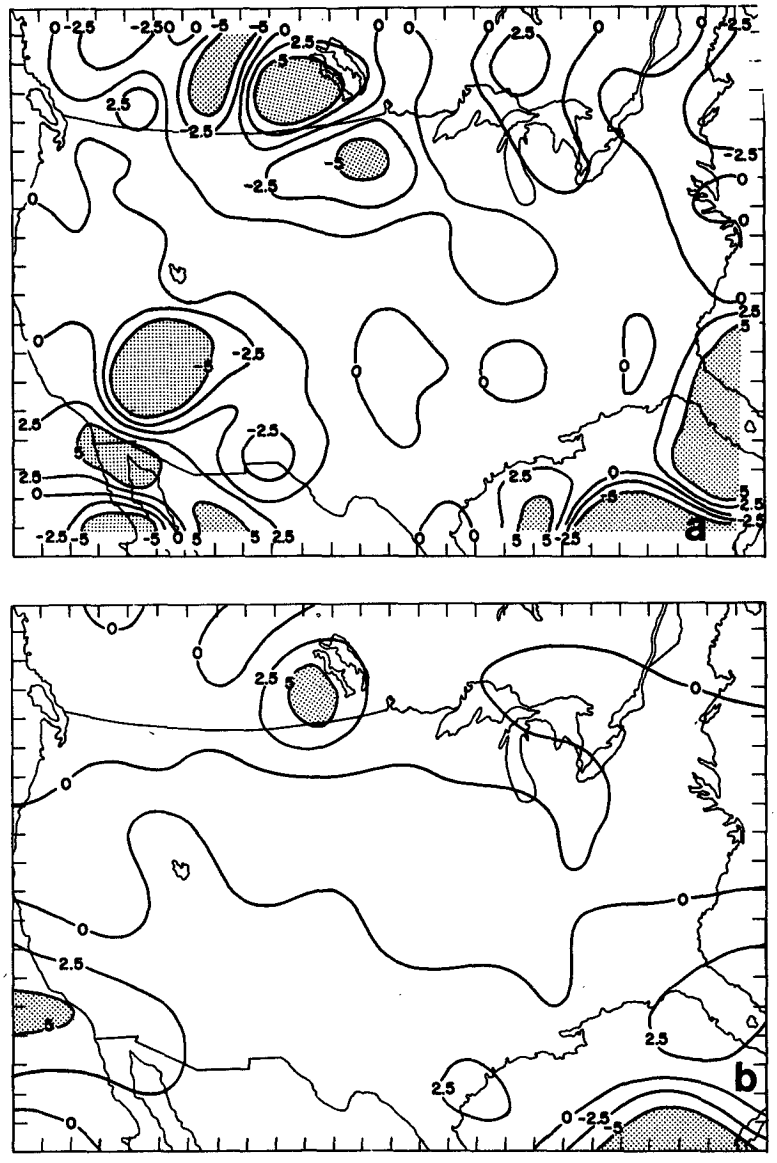

FIG. 8. Divergence times 10^{-6} s^{-1}, calculated from approximation to the defined streamfunction; shading denotes magnitudes in excess of 5.0×10^{-6} s^{-1}. (a) Differential definition from component analysis, (b) direct evaluation via line integral.

3. Inversion of the derived field to obtain the winds

a. Comments on boundary conditions

According to the Helmholtz theorem, the horizontal wind **v** can be partitioned into irrotational and nondivergent components

$$\mathbf{v} = \nabla_H \chi + \mathbf{k} \times \nabla_H \psi, \tag{6}$$

where χ is the velocity potential, ψ the streamfunction and ∇_H the horizontal gradient operator. Velocity potential and streamfunction are related to the divergence (D) and vertical component of vorticity (ξ) by

$$\nabla_H^2 \chi = D, \tag{7}$$

$$\nabla_H^2 \psi = \xi. \tag{8}$$

If global values of D and ξ are known or measured directly, **v** can be determined within an additive constant.

When the domain is restricted, **v** becomes dependent upon boundary conditions. From (6) it is

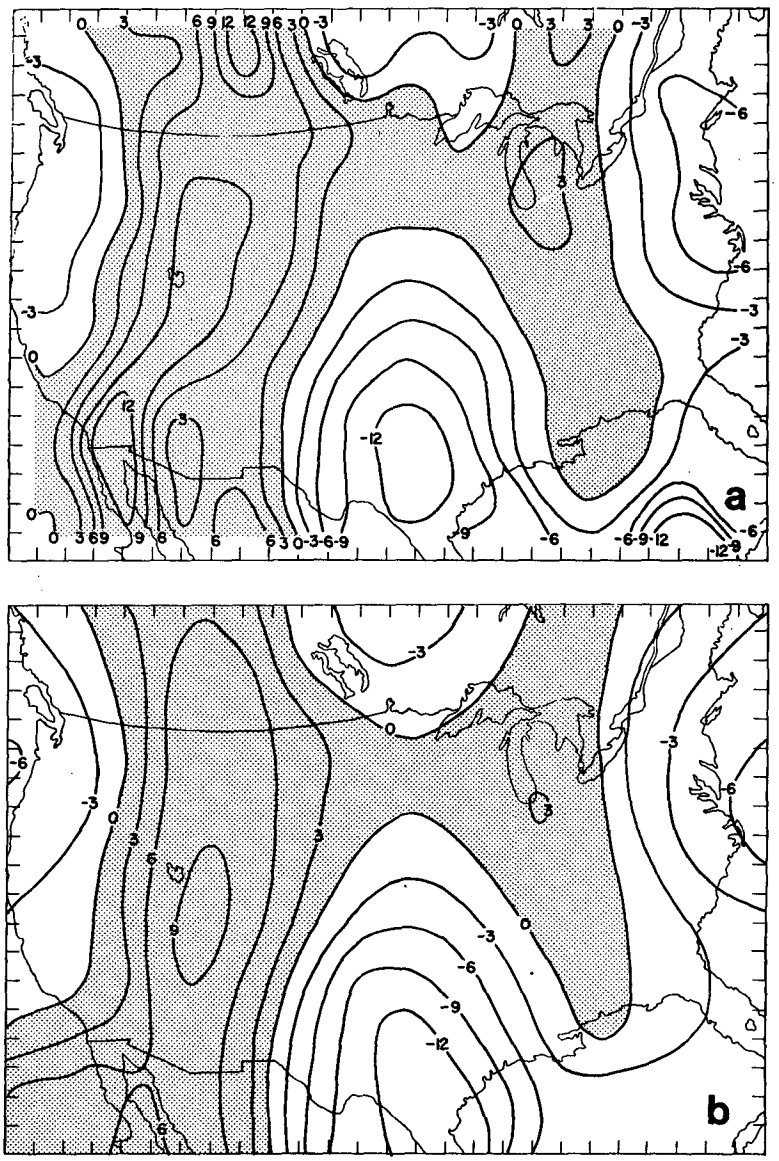

FIG. 9. Vorticity times 2.5×10^{-6} s^{-1}, calculated from approximation to the defined streamfunction; shading denotes positive values. (a) Differential definition from component analysis, (b) direct evaluation via line integral.

obvious that the boundary wind must satisfy

$$\mathbf{n}\cdot\mathbf{v} = \frac{\partial\chi}{\partial n} - \frac{\partial\psi}{\partial t}, \tag{9}$$

$$\mathbf{t}\cdot\mathbf{v} = \frac{\partial\psi}{\partial n} + \frac{\partial\chi}{\partial t}, \tag{10}$$

when $\mathbf{n}$ and $\mathbf{t}$ are normal and tangential unit vectors along the boundary curve.

Sangster (1960) has shown that the specification of a constant velocity potential around the boundary is tantamount to minimizing the total kinetic energy of the nondivergent wind field and maximizing that of the irrotational one. The reality of this particular energy partitioning is quite dependent upon the geometry (scale) of the flow being considered.

Integrating (6) over the domain and applying Green's theorem yields

$$\iint_S \mathbf{v}\,d\sigma = \oint_\Gamma \mathbf{n}\chi\,dt + \oint_\Gamma \psi\,d\mathbf{t}. \tag{11}$$

Thus, as pointed out by Stephens (1968), a constant boundary condition in χ (or ψ) requires that the irrotational (or nondivergent) velocity be equal to the observed velocity. Further, any meaningful specification of boundary conditions on χ and ψ,

whether Dirichlet [via Eq. (11)], Neumann [via. Eqs. (9) and (10)], or mixed, requires a foreknowledge of the previously mentioned partitioning (Shukla and Saha, 1974). Such knowledge is generally not available.

b. Variational adjustment of a preliminary wind analysis

By making an adjustment to a preliminary wind analysis (generally obtained via component interpolation), it is possible to obtain a final wind field that has the "measured" divergence and vorticity content. At the same time, the difference between the preliminary wind analysis and the final result is also minimized. This adjustment can be cast as a variational problem (Sasaki, 1970). The required functional is

$$J = \iint_S [(\mathbf{v} - \tilde{\mathbf{v}})^2 + \lambda_1(\mathbf{k}\cdot\nabla \times \mathbf{v} - \tilde{\xi}) + \lambda_2(\nabla\cdot\mathbf{v} - \tilde{D})]d\sigma, \quad (12)$$

where:

$\mathbf{v}(x,y)$	final analyzed horizontal vector wind
$\tilde{\mathbf{v}}(x,y)$	preliminary horizontal vector wind
$\tilde{\xi}(x,y)$	measured vertical component of vorticity
$\tilde{D}(x,y)$	measured horizontal divergence
λ_1, λ_2	Lagrange multipliers.

After setting the first variation of Eq. (12) to zero and applying Green's theorem, the Euler-Lagrange (EL) equations are found to be

$$\mathbf{v} - \tilde{\mathbf{v}} = \tfrac{1}{2}[\nabla\lambda_2 + \mathbf{k} \times \nabla\lambda_1], \quad (13)$$

$$\nabla\cdot\mathbf{v} = \tilde{D}, \quad (14)$$

$$\mathbf{k}\cdot\nabla \times \mathbf{v} = \tilde{\xi}. \quad (15)$$

The associated natural boundary conditions (NBC) are

$$\oint_\Gamma \lambda_1\delta\mathbf{v}\cdot d\mathbf{t} = 0, \quad (16)$$

$$\oint_\Gamma \lambda_2\mathbf{k}\cdot\delta\mathbf{v} \times d\mathbf{t} = 0. \quad (17)$$

By combining Eqs. (13), (14) and (15), it is found that the Lagrange multipliers must satisfy

$$\nabla^2\lambda_1 = 2[\tilde{\xi} - \mathbf{k}\cdot\nabla \times \mathbf{v}], \quad (18)$$

$$\nabla^2\lambda_2 = 2[\tilde{D} - \nabla\cdot\mathbf{v}]. \quad (19)$$

The problem reduces to solving Eqs. (18) and (19) under the constraints of the NBC [Eqs. (16) and (17)].

There are myriad potential ways that the NBC can be satisfied. However, by considering the integral constraints upon the system, the options become limited. First note

$$\iint_S \nabla^2\lambda_2 d\sigma = 2\iint_S [\tilde{D} - \nabla\cdot\tilde{\mathbf{v}}]d\sigma = 2\oint_\Gamma (\mathbf{v} - \tilde{\mathbf{v}})\cdot\mathbf{n}dt = \oint_\Gamma \frac{\partial\lambda_2}{\partial n}\,dt, \quad (20)$$

$$\iint_S \nabla^2\lambda_1 d\sigma = 2\iint_S [\tilde{\xi} - \mathbf{k}\cdot\nabla \times \tilde{\mathbf{v}}]d\sigma = 2\oint_\Gamma (\mathbf{v} - \tilde{\mathbf{v}})\cdot d\mathbf{t} = \oint_\Gamma \frac{\partial\lambda_1}{\partial n}\,dt. \quad (21)$$

That is, the difference between the measured divergence (or vorticity) and that obtained via differentiation of the wind field is totally contained in the normal derivative of λ_2 (or λ_1) across the boundary, or equivalently in the change of the normal (or tangential) wind component at the boundary. Thus, Neumann conditions require a preknowledge of the wind field along the boundary.

Additional elucidation of the boundary conditions comes from the requirements that

$$\iint_S \nabla\lambda_2 d\sigma = \iint_S [2(\mathbf{v} - \tilde{\mathbf{v}}) - \mathbf{k} \times \nabla\lambda_1]d\sigma = \oint_\Gamma \lambda_2\mathbf{n}dt, \quad (22)$$

$$\iint_S \nabla\lambda_1 d\sigma = \iint_S \{\mathbf{k} \times [2(\mathbf{v} - \tilde{\mathbf{v}}) - \nabla\lambda_2]\}d\sigma = \oint_\Gamma \lambda_1\mathbf{n}dt. \quad (23)$$

Eqs. (22) and (23) emphasize that the two Lagrange multipliers are not independent; the specification of one multiplier along the boundaries puts internal restrictions upon the other multiplier. This suggests that use of any exotic boundary specification for the multipliers may be self-defeating. Consequently, the simplest specification which satisfies the NBC, i.e.,

$$\lambda_1\big|_\Gamma = \lambda_2\big|_\Gamma = 0, \quad (24)$$

seems to be reasonable. The implications of this boundary condition can be seen by noting that Eq. (13) requires

$$\iint_S (\mathbf{v} - \tilde{\mathbf{v}})d\sigma = \iint_S \tfrac{1}{2}[\nabla\lambda_2 + \mathbf{k} \times \nabla\lambda_1]d\sigma = \tfrac{1}{2}\oint_\Gamma \lambda_2\mathbf{n}dt + \tfrac{1}{2}\oint_\Gamma \lambda_1 d\mathbf{t}. \quad (25)$$

Thus, when condition (24) is used, the total area-averaged velocity of the final wind analysis is equal to that of the preliminary one. This restriction is not as harmful as it first appears since, at the expense of noise in the analyzed field (and thus the derived

TABLE 1. Statistical error analysis comparison between Gaussian interpolation and variational adjustment of a preliminary wind analysis.

	Variational wind adjustment		Gaussian	
	rms	Algebraic	rms	Algebraic
u-component	0.50	0.09	0.51	0.01
v-component	0.35	0.08	1.18	−0.11
Speed	0.46	0.01	0.79	−0.40
Vector	0.61	0.46	1.28	1.12

quantities), it is possible to force the preliminary wind analysis to within about 10–15% of the raw observations (Endlich and Clark, 1963). Because this noise is in the "first guess" field, it will not seriously contaminate the final analysis.

To show the validity of variational wind inversion technique, the Miyakoda streamfunction [Eq. (5)] is again used. The defined vorticity ($\xi = \nabla^2\psi$) and divergence ($D = 0.0$) are used as the measured values. The "first guess" wind field ($\tilde{\mathbf{v}}$) is computed via the same technique employed in the last section. Using the improved second-order finite difference analogue to the Laplacian developed by Schaefer (1977), Eqs. (13), (18) and (19) under boundary conditions (24) are numerically solved for the vector wind field ($\mathbf{v}$).

The wind field obtained via the variational technique shows marked improvement over the one obtained by simple Gaussian interpolation of components. For illustration, consider the v-component field (Fig. 10). While the gross features of the defined, variational and interpolated fields are in general agreement, details of the pattern and magnitudes of the relative extrema in the variational solution give a more realistic representation of the true v field.

To compare the two analysis techniques statistically, bilinear interpolation is used to obtain wind estimates at the observation points from the gridded fields. This method of comparison is chosen to provide a standard technique that can be applied when the true field is unknown. Preliminary testing has shown that the statistics obtained in this way are virtually identical to those obtained directly from the gridded data, when theoretical fields are used. Statistics from the comparison for the 62 data points interior to the variational analysis grid are given in Table 1. Vector error is defined by Shukla and Saha (1974) as

$$E \equiv [(u_o - u_a)^2 + (v_o - v_a)^2]^{1/2}, \qquad (26)$$

where the subscript o stands for observed and a for analyzed. In each case, except the algebraic u-component, the error is less for the variational wind retrieval than for the objective component interpolation. Thus, not only does this wind retrieval technique preserve the original divergence and vorticity fields, but it also gives a statistically improved wind field analysis.

c. *Variational adjustment of the divergence and vorticity*

While the variational adjustment of a preliminary wind analysis yields a very accurate solution, it is computationally quite complicated. An alternative exists which is more economical in terms of computer core storage and eliminates the need for numerical differentiation [Eq. (13)], which is required to find the grid-point wind components after solution of the two Poisson-type equations [(18) and (19)]. This method finds a wind whose divergence and vorticity are as close to those measured as possible under the restrictions of a boundary specification of the winds. While this technique is less accurate than the previous one, it is sufficient for many applications.

As before, the method can be expressed as a variational problem, but the restriction that the difference between preliminary and analyzed winds also be minimal is removed. The required functional is simply

$$I = \iint_S [(\mathbf{k}\cdot\nabla \times \mathbf{v} - \tilde{\xi})^2 + (\nabla\cdot\mathbf{v} - \tilde{D})^2]d\sigma. \qquad (27)$$

Taking the first variation of Eq. (27) and applying Green's theorem yields

$$\tfrac{1}{2}\delta I = \iint_S \{-\delta\mathbf{v}\cdot\nabla(\nabla\cdot\mathbf{v} - \tilde{D}) + \mathbf{k}\cdot\delta\mathbf{v} \times \nabla(\mathbf{k}\cdot\nabla \times \mathbf{v} - \tilde{\xi})\}d\sigma + \oint_\Gamma \{[(\nabla\cdot\mathbf{v} - \tilde{D})\mathbf{n} + (\mathbf{k}\cdot\nabla \times \mathbf{v} - \tilde{\xi})\mathbf{t}]\cdot\delta\mathbf{v}\}dt. \qquad (28)$$

The difference between the final and the measured divergence (vorticity) is minimal when both integrals vanish. The EL equations arise from the surface integral while the NBC come from the line integral.

Breaking the surface integral into components shows the EL equations are equivalent to

$$m^2\left[\frac{\partial^2}{\partial x^2}\left(\frac{u}{m}\right) + \frac{\partial^2}{\partial y^2}\left(\frac{u}{m}\right)\right] = m^2\left[\frac{\partial}{\partial x}\left(\frac{\tilde{D}}{m^2}\right) - \frac{\partial}{\partial y}\left(\frac{\tilde{\xi}}{m^2}\right)\right] = \nabla^2\left(\frac{u}{m}\right), \qquad (29)$$

$$m^2\left[\frac{\partial^2}{\partial x^2}\left(\frac{v}{m}\right) + \frac{\partial^2}{\partial y^2}\left(\frac{v}{m}\right)\right] = m^2\left[\frac{\partial}{\partial x}\left(\frac{\tilde{\xi}}{m^2}\right) + \frac{\partial}{\partial y}\left(\frac{\tilde{D}}{m^2}\right)\right] = \nabla^2\left(\frac{v}{m}\right), \qquad (30)$$

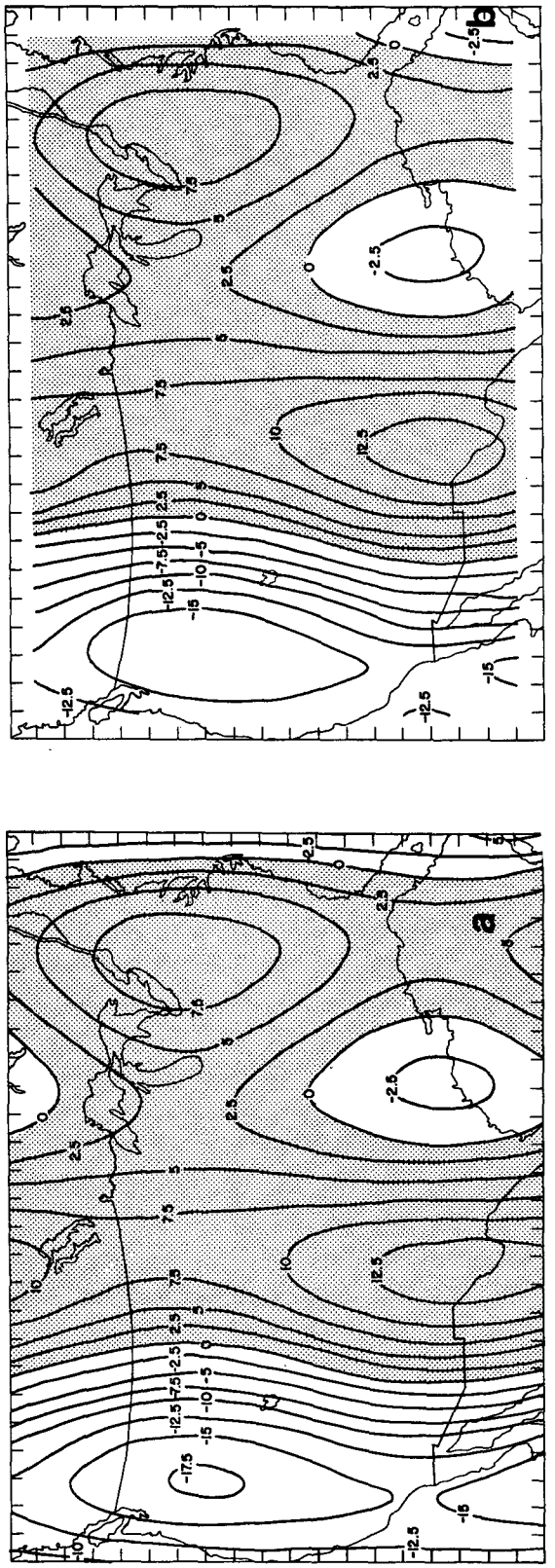

FIG. 10. v-component (m s^{-1}) analysis corresponding to defined streamfunction; shading denotes positive values. (a) Theoretical field, (b) field obtained from a variational adjustment of a preliminary wind analysis, (c) preliminary wind analysis obtained by component interpolation.

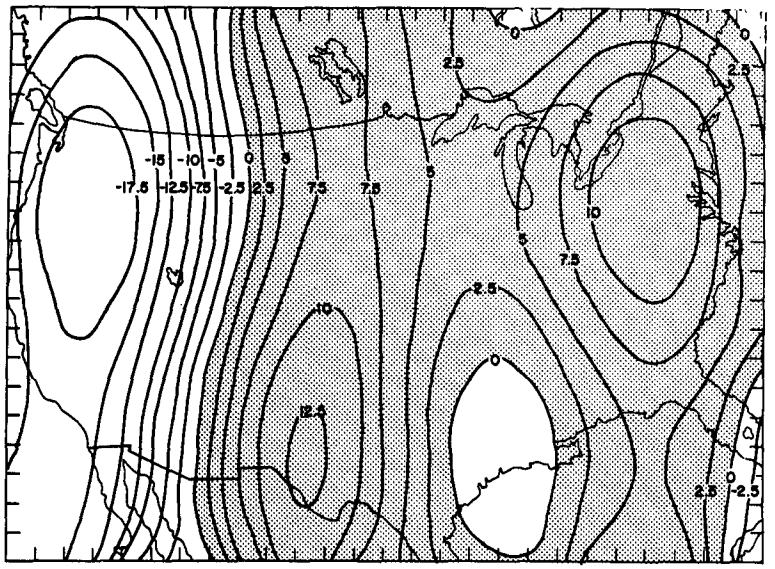

FIG. 11. v-component (m s^{-1}) analysis corresponding to defined streamfunction, obtained by variational adjustment of the divergence and vorticity; shading denotes positive values.

TABLE 2. Statistical error analysis comparison between Gaussian interpolation and variational adjustment of divergence and vorticity.

	Variational wind adjustment		Gaussian	
	rms	Algebraic	rms	Algebraic
All data points (73) interior to domain				
u-component	0.47	0.20	0.53	0.00
v-component	1.80	0.48	1.21	0.02
Speed	1.06	0.63	0.79	−0.34
Vector	1.86	1.56	1.32	1.15
Excluding data within one grid increment of boundary, 62 data points remain				
u-component	0.45	0.24	0.51	0.01
v-component	1.67	0.50	1.18	−0.11
Speed	1.01	0.63	0.79	−0.40
Vector	1.73	1.47	1.28	1.13
Excluding data within two grid increments of boundary, 51 data points remain				
u-component	0.37	0.24	0.49	−0.03
v-component	1.60	0.65	1.24	−0.05
Speed	.99	0.66	0.85	−0.43
Vector	1.64	1.39	1.34	1.20
Excluding data within three grid increments of boundary, 46 data points remain				
u-component	0.35	0.24	0.48	−0.06
v-component	1.33	0.40	1.27	−0.07
Speed	0.84	0.55	0.85	−0.50
Vector	1.38	1.22	1.36	1.21

where m is the metric coefficient determined by the analysis grid geometry. These are Poisson equations for the wind components and can be numerically solved under the restrictions of the NBC.

The NBC will be satisfied when either

$$(\nabla\cdot\mathbf{v} - \tilde{D})\big|_\Gamma = (\mathbf{k}\cdot\nabla\times\mathbf{v} - \tilde{\xi})\big|_\Gamma = 0, \quad (31)$$

or

$$\delta\mathbf{v}\big|_\Gamma = 0. \quad (32)$$

Because of the interrelationship between $\nabla\cdot\mathbf{v}$ and $\mathbf{k}\cdot\nabla\times\mathbf{v}$, Eq. (31) does not provide viable boundary conditions. Thus, solution requires condition (32). This will be satisfied if the winds along the boundary are specified via an independent analysis.

The validity of this wind retrieval technique is tested using the same experiment employed in the last section. The pattern in the analyzed component fields is similar to that of the analytically defined data. Fig. 11 shows the retrieved v-component; this should be compared to Fig. 10a. Gradients in the retrieved field are quite similar to those which actually exist. However, definite discrepancies between the defined field and the analyzed field are present, especially near the boundaries. Error statistics obtained by comparing the analyzed field to the observations for this method and for the Gaussian component analysis scheme are given in Table 2. As the domain of comparison is moved away from the boundary (Shukla and Saha, 1974), the variational technique improves relative to the standard method.

The vorticity of the final wind analysis is shown

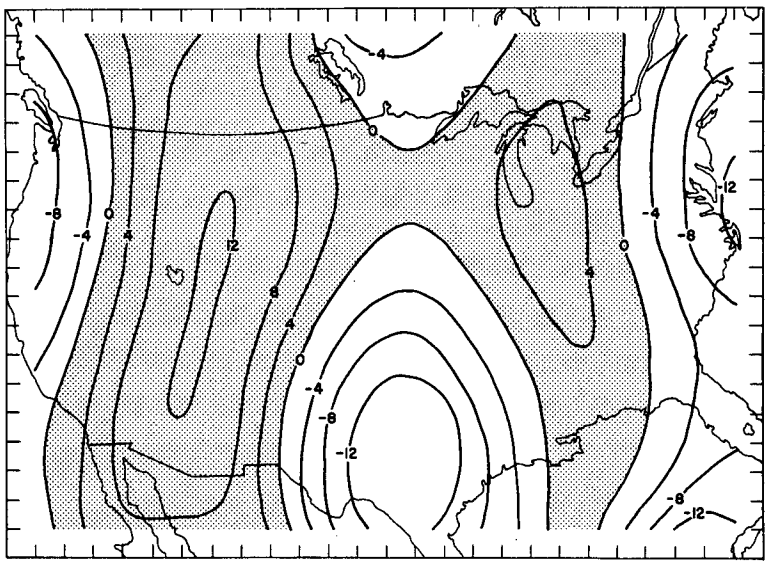

FIG. 12. Vorticity times 2.5×10^{-6} s^{-1}, obtained by variational adjustment; shading denotes positive values.

in Fig. 12. This compares quite favorably with the actual vorticity (Fig. 7b). The boundary effect is dramatically shown by the analyzed divergence field (Fig. 13). Near the center of the domain, the analyzed divergence is effectively zero (remember the true divergence is zero everywhere); however, as the boundaries are approached, multiple fallacious maxima and minima appear.

The quality of the analysis produced by this technique can be enhanced by increasing the quality of the wind analysis along the boundary. Nevertheless, even with the present boundary analysis, when the outer three grid rows are omitted, a marked improvement in the quality of the estimates for vorticity (Fig. 12 vs Fig. 9a) and divergence (Fig. 13 vs 8a) occurs for this variational technique, compared to the Gaussian interpolation, with virtually no increase in the rms vector error (0.02 m s^{-1}).

4. Application to real meteorological data

When observed data are analyzed, it is no longer possible to declare one analysis technique definitely

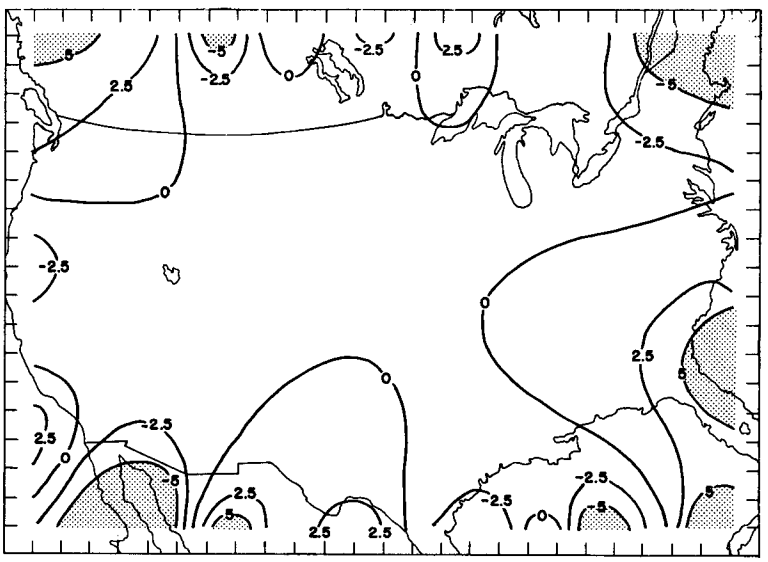

FIG. 13. Divergence times 10^{-6} s^{-1}, obtained by variational adjustment; shading denotes magnitudes in excess of 5×10^{-6} s^{-1}.

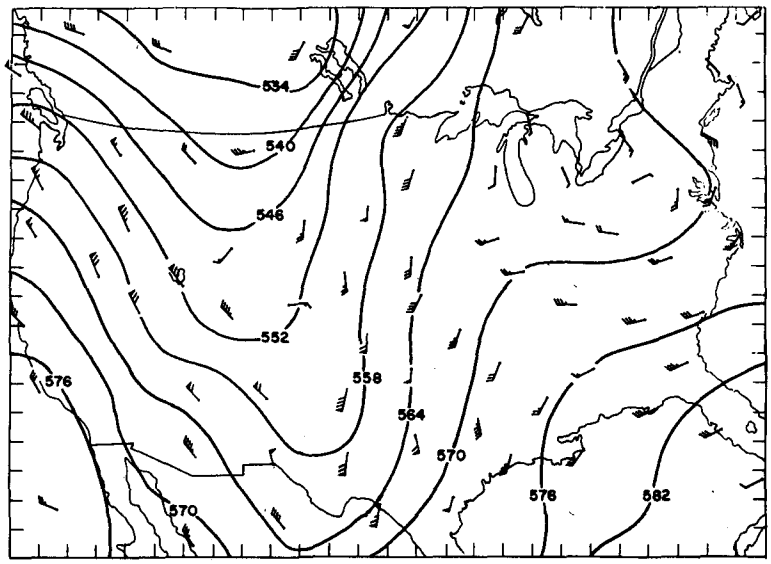

FIG. 14. Isophypse analysis (dam) for 1200 GMT 8 November 1977 and wind observations (flag = 25 m s^{-1}, barb = 5 m s^{-1}, half barb = 2.5 m s^{-1}).

better than another, as true divergence and vorticity fields are unknown. Also, since a synoptic-scale wind analysis is desired, measured wind vectors do not necessarily represent the synoptic-scale field (Shapiro, 1972). However, if divergence and vorticity fields produced via the integral technique are dynamically consistent with the geopotential field, results of the preceding analytic experiments allow us to assert that the variational technique produces a viable approximation to the true synoptic-scale wind field.

The example to be examined consists of the 50 kPa data for 1200 GMT 8 November 1977 (Fig. 14). A long-wave trough is situated along the Rocky Mountains with short waves positioned over the Great Basin and along 105°W. A minor short-wave trough is also present in the vicinity of the Potomac River. Considerable wind shear and velocity convergence are suggested in association with major trough.

The divergence field produced by the component calculation (Fig. 15a) indicates a relative convergence maximum in the eastern portion of the long-wave trough. In the direct analysis of divergence (Fig. 15b) this maximum is replaced by a saddle point, implying that the rotational component of the flow dominates the divergent one around the base of the trough. This difference in representation is also evident in the vorticity analysis. The component definition (Fig. 16a) indicates two distinct positive vorticity centers internal to the system, one with each short wave. In contrast, the integral computation (Fig. 16b) suggests that these minor short waves are not significant and locates one positive center at the approximate base of the long wave. The 50 kPa analysis 12 h later (not shown) shows little evidence of these short waves but, rather, reveals an eastward progression of the major trough.

As an extremely crude approximation, one would expect convergent (divergent) areas at 50 kPa to correspond to regions of negative (positive) vorticity advection (Saucier, 1955, p. 355). This relationship is more nearly valid for the line integral analysis than when the divergence and vorticity are computed from derivatives. For example, the line integral divergence shows a greater tendency for a north-south divergence axis east of the trough, in the region of positive vorticity advection. Thus, there is a heuristic consistency in the proposed analysis method which is lacking in a more conventional objective wind interpolation technique.

Wind component fields obtained via variational adjustment of a preliminary wind analysis are shown in Fig. 17. Also indicated are the changes to the Gaussian wind component analysis. Except in the immediate neighborhood of the trough, changes are less than 5 m s^{-1}. The only major alternation to the u-component field is in New Mexico where the "westerly" component is reduced by about 5 m s^{-1}. This reduction is a reflection of decreased convergence along the axis of the trough and points to an inconsistency between the wind observation at Albuquerque and the surrounding stations.

The only significant v-component change (reduction of about 6 m s^{-1}) appears in west Texas, re-

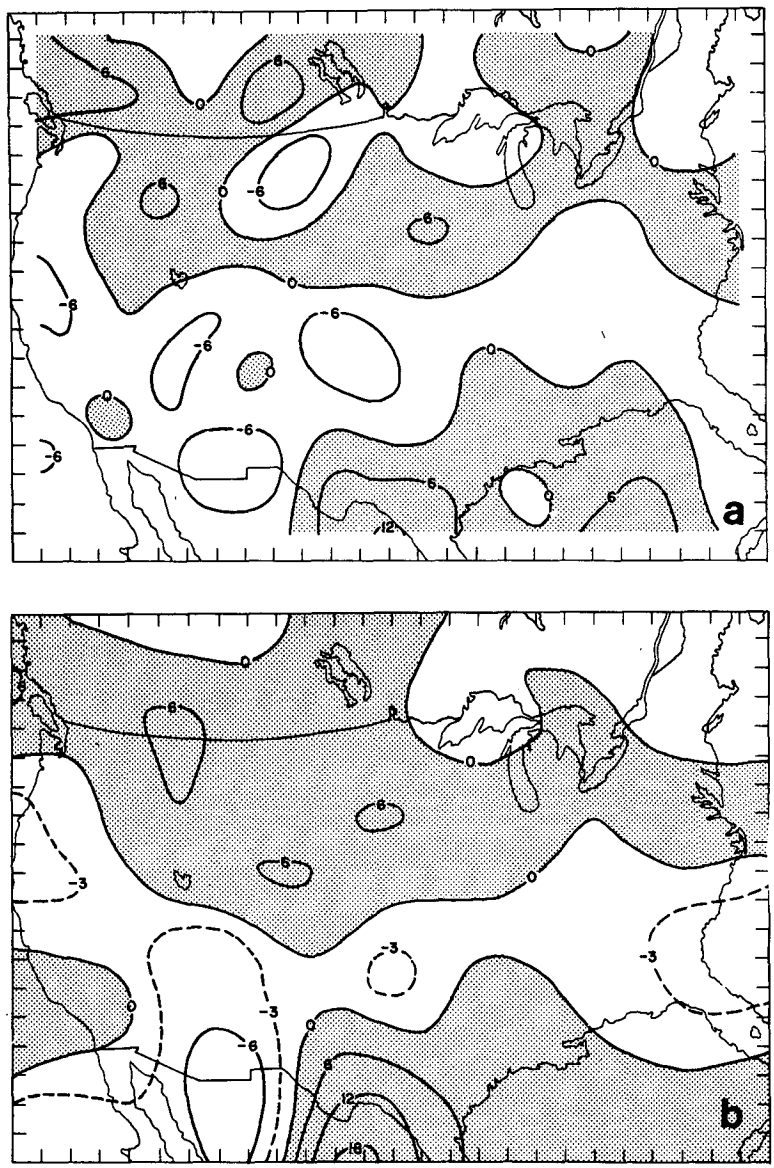

FIG. 15. Divergence times 2.0×10^{-6} s^{-1} at 50 kPa, 1200 GMT 8 November 1977; shading denotes positive values. (a) Differential definition from component analysis, (b) direct evaluation via line integral.

flecting the spectral restriction of the analyses (wind, divergence and vorticity) to the synoptic scale. This change results from the decreased emphasis placed on the short waves by the direct analysis, reducing the v-component wind shear across the trough (vorticity).

5. Summary

The essential problem of the non-uniqueness of vector interpolation has been investigated, with applications to meteorological wind fields in mind. Since horizontal divergence and the vertical component of relative vorticity are fundamental aspects of the horizontal vector wind field, it is clearly desirable to preserve these properties during any interpolation of the winds. To this end, a method of evaluating divergence and vorticity directly from wind observations has been developed. The technique is applied to two analytically defined fields to show that the results obtained can improve upon those obtained via component differentiation of gridded winds. While specific results may be dependent upon the interpolation technique em-

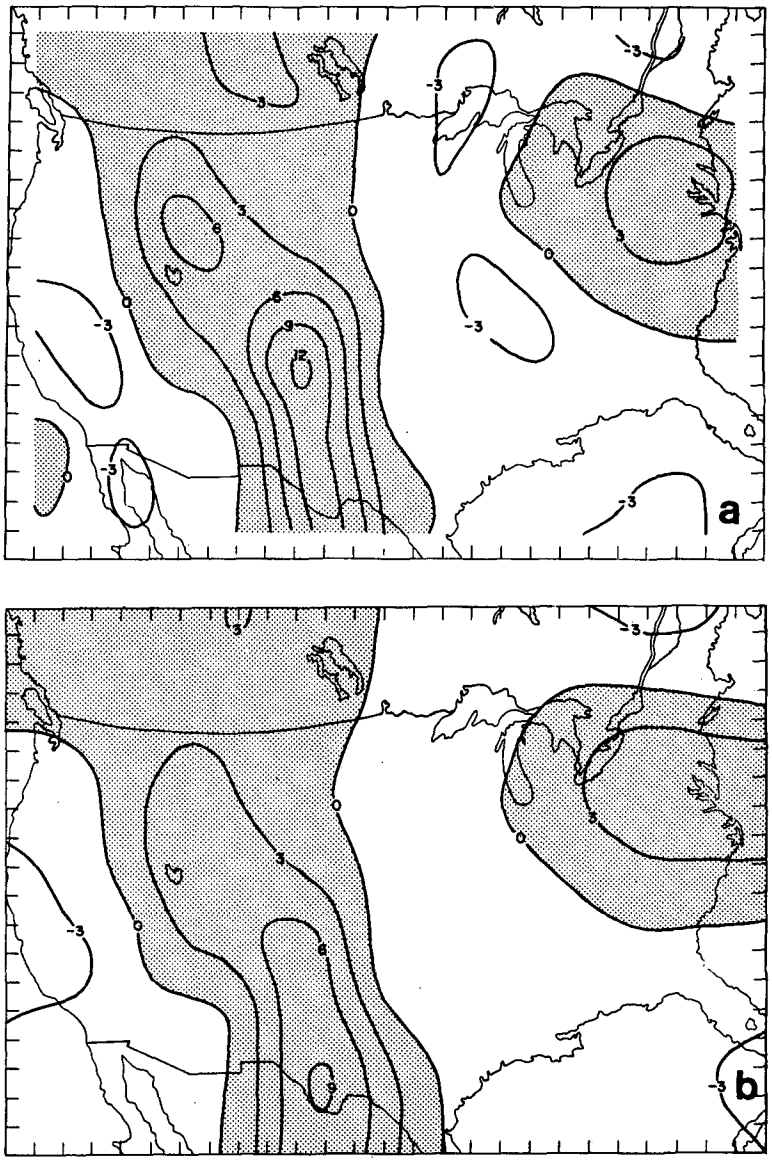

FIG. 16. Vorticity times 10^{-5} s^{-1} at 50 kPa, 1200 GMT 8 November 1977; shading denotes positive values. (a) Differential definition from component analysis, (b) direct evaluation via line integral.

ployed, the same algorithm is used to grid divergence and vorticity "observations" as for the wind components. Thus, this aspect of the problem does not detract from the generality of the results.

Having available what are effectively "observed" fields of divergence and vorticity makes the problem of reconstructing the wind field from these quantities somewhat different from previous treatments. Using variational principles, two methods for retrieving gridded wind fields (interpolation in a vector space) are developed. One method forces the analyzed wind field to have the measured divergence and vorticity while conserving the area-averaged velocity of a preliminary analysis. The second method minimizes the deviations in the wind field's divergence and vorticity from the "true" values while maintaining the boundary wind component values from a preliminary analysis. Both of these techniques are applied to an analytic field and results suggest that the reconstructed winds are markedly better than those produced by a typical objective analysis.

The entire analysis package is applied to an actual meteorological data set. The most striking fea-

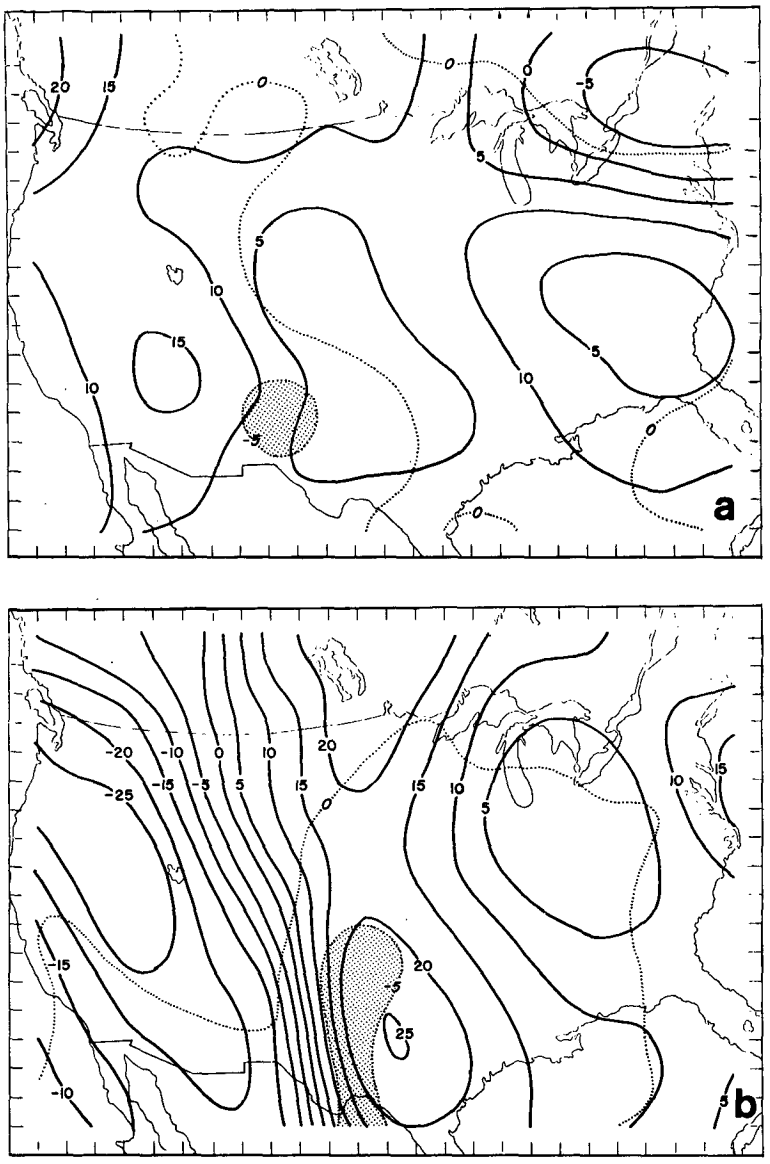

FIG. 17. Wind analysis (m s^{-1}) at 50 kPa, 1200 GMT 8 November 1977. Solid lines indicate retrieved winds via variational adjustment of preliminary analysis; dotted lines denote the changes (m s^{-1}) to the preliminary analysis; shading denotes changes in excess of 5 m s^{-1}. (a) u-component, (b) v-component.

ture of the results is the consistency between fields. The divergence, vorticity and wind component analyses all contain approximately the same degree of roughness and from heuristic arguments are dynamically compatible.

Acknowledgments. The authors would like to express their appreciation to their colleagues Dr. Richard McNulty and Mr. Leslie Lemon of the Techniques Development Unit for their assistance in the development in the concepts presented. Ms. Sandra Boyse and Ms. Margaret Coonfield typed the manuscript.

REFERENCES

Barnes, S. L., 1964: A technique for maximizing details in numerical weather map analysis. *J. Appl. Meteor.*, **3**, 396–409.

Bedient, M. A., and J. Vederman, 1964: Computer analysis and forecasting in the tropics. *Mon. Wea. Rev.*, **92**, 565–577.

Bellamy, J. C., 1949: Objective calculations of divergence, vertical velocity and vorticity. *Bull. Amer. Meteor. Soc.*, **30**, 45–49.

Blackman, R. B., and J. W. Tukey, 1958: *The Measurement of Power Spectra*. Dover, 190 pp.

Ceselski, B. F., and L. L. Sapp, 1975: Objective wind field analysis using line integrals. *Mon. Wea. Rev.*, **103**, 89–100.

Doswell, C. A. III, 1977: Obtaining meteorologically significant surface divergence fields through the filtering property of objective analysis. *Mon. Wea. Rev.*, **105**, 885–892.

Eddy, A., 1964: The objective analysis of horizontal wind divergence fields. *Quart. J. Roy. Meteor. Soc.*, **90**, 424–440.

Endlich, R. M., and J. R. Clark, 1963: Objective computation of some meteorological variables. *J. Appl. Meteor.*, **2**, 66–81.

Hamming, R. W., 1962: *Numerical Methods for Scientists and Engineers*. McGraw-Hill, 411 pp.

Hawkins, H. F., and S. L. Rosenthal, 1965: On the computation of stream functions from the wind field. *Mon. Wea. Rev.*, **93**, 245–252.

Leary, C., and R. O. R. Y. Thompson, 1973: Shortcomings of an objective analysis scheme. *J. Appl. Meteor.*, **12**, 589–594.

Levinson, N., and R. M. Redheffer, 1970: *Complex Variables*. Holden-Day, 429 pp.

Milne-Thomson, L. M., 1968: *Theoretical Hydrodynamics*, 5th ed. Macmillan, 743 pp.

Miyakoda, K., 1963: Contribution to the numerical weather—computation with finite difference. *Japan J. Geophys.*, **3**, 75–190.

Morel, P., and G. Necco, 1973: Scale dependence of the 200 mb divergence inferred from EOLE data. *J. Atmos. Sci.*, **30**, 909–921.

Sangster, W. E., 1960: A method of representing the horizontal pressure force without reduction of station pressures to sea level. *J. Meteor.*, **17**, 166–176.

Sasaki, Y., 1970: Some basic formalisms in numerical variational analysis. *Mon. Wea. Rev.*, **98**, 875–883.

Saucier, W. J., 1955: *Principles of Meteorological Analysis*. University of Chicago Press, 438 pp.

Schaefer, J. T., 1977: An improved second order finite difference analogue for the Laplacian operator. *J. Meteor. Soc. Japan*, **55**, 511–517.

Schwartz, M., S. Green and W. A. Rutledge, 1960: *Vector Analysis*. Harper, 556 pp.

Shapiro, R., 1972: Information loss and compensation in linear interpolation. *J. Comput. Phys.*, **10**, 65–84.

Shukla, J., and K. R. Saha, 1974: Computation of non-divergent stream-function and irrotational velocity potential from the observed winds. *Mon. Wea. Rev.*, **102**, 419–425.

Shuman, F. G., and J. B. Hovermale, 1968: An operational six-layer primitive equation model. *J. Appl. Meteor.*, **7**, 525–547.

Stephens, J. J., 1968: Variational resolution of wind components. *Mon. Wea. Rev.*, **96**, 229–231.

Williams, R. J., 1976: Surface parameters associated with tornadoes. *Mon. Wea. Rev.*, **104**, 540–545.